Available online at www.sciencedirect.com

ScienceDirect

Energy Procedia 55 (2014) 241 – 246

Energy Procedia

4th International Conference on Silicon Photovoltaics, SiliconPV 2014

The potential advantage of industrially processed boron emitters compared to phosphorus emitters

Yuji Komatsu[a,*], Ard H. G. Vlooswijk[b], Peter R. Venema[b], Ingrid G. Romijn[a]

[a]*ECN Solar Energy, P.O.Box 1, 1755ZG Petten, the Netherlands*
[b]*Tempress Systems BV, Radeweg 31, 8171MD Vaassen, the Netherlands*

Abstract

A boron emitter that is transferrable to mass production is compared to a phosphorus emitter of industrial standard and a phosphorus emitter with reduced phosphorus concentration, on the viewpoints of the doping profiles, emitter saturation current (J_{0E}), and internal quantum efficiency at shorter wavelength (= blue IQE). The doping profiles are characterized considering active and inactive dopant, and including the doping source before HF treatment. We found boron atoms are segregated towards the doping source while phosphorus segregates towards the emitter, which could explain the absence of inactive dopant in boron emitters as opposed to a substantial amount of inactive dopant in phosphorus emitters. It was also found that inactive phosphorus is still present even down to 1×10^{19} cm^{-3} also for the lightly doped emitter. The boron emitter showed the highest blue IQE probably due to the absence of both inactive dopant and heavy doping above 1×10^{20} cm^{-3}. On the other hand, 10 mV V_{oc} gain of the phosphorus emitters by decreasing J_{0E} from 180 to 45 fA/cm^2 implied the possibility of V_{oc} improvement also for the boron emitter by reducing J_{0E} which is 97 fA/cm^2 at present.

Peer-review under responsibility of the scientific committee of the SiliconPV 2014 conference

Keywords: emitter; BBr_3; $POCl_3$; doping profile; SIMS; ECV; BSG; PSG

1. Introduction

The advantage of n-type substrates for silicon solar cells has been exhibited in various publications [1,2]. High efficiency IBC and HIT cells are manufactured using n-type material [3,4]. Even for the traditional structure with

* Corresponding author. Tel.: +31-224-56-4303; fax: +31-224-56-8214.
E-mail address: komatsu@ecn.nl

Peer-review under responsibility of the scientific committee of the SiliconPV 2014 conference
doi:10.1016/j.egypro.2014.08.074

homogeneous front-side emitter and back surface field, and contacts on both sides applied by printing metal paste, solar cells industrially processed from n-type material demonstrate higher efficiencies. For example, 20.2% average cell efficiency has been achieved by our group [5]. The approach of this work is to compare the boron emitter in the mentioned work [5], which is transferrable to mass production, to phosphorus emitters of industrial standard and of reduced phosphorus concentration, and find out the difference in performance among these boron and phosphorus emitters.

2. Experiments

2.1. Doping process

Phosphorus and boron are normally chosen as doping elements for the front side emitter due to their high solid solubility [6,7], which will render a sufficiently low sheet resistance (< 100 Ω/sq.) for thin (< 0.5 μm) doped layers. The practical approach to form the emitter in mass production is thermal diffusion, and the most popular method is using a quartz tube furnace with liquid source —— $POCl_3$ for phosphorus and BBr_3 for boron —— whose vapour is conveyed by inert gas bubbling [8,9]. Since both of the liquid sources are supplied with O_2 to thermally decompose the gasses, silicon oxide films containing the doping elements are grown on the silicon surface as by-product which are called phosphosilicate glass (PSG) and borosilicate glass (BSG).

Mass production of emitters requires uniform and reproducible manufacturing with high throughput. The most successful method to achieve uniform emitters reproducibly for all cases of across-wafer, wafer-to-wafer, and batch-to-batch is to apply an excessive amount of doping source resulting in dopant concentrations in the Si up to or even above the solid solubility. Otherwise, the peak doping concentration is likely to vary which causes diverse doping profiles across the wafer, wafer-to-wafer, and/or batch-to-batch resulting in widely scattered solar cell performances, which is not favorable in mass production.

In this work, we used an industry-scale 3-stack tube furnace for $POCl_3$ and BBr_3, each of which is equipped with 400 slots for loading 156×156 mm² wafers in its 1000 mm-long temperature flat zone.

2.2. Characterization

In this work, we characterized doping profiles by D-SIMS (dynamic secondary ion mass spectroscopy) using ToF-SIMS (Time-of-Flight SIMS) at Philips Innovation Services [10] and ECV (electrochemical capacitance-voltage) supplied by WEP CVP21 [11]. The former is capable to detect the chemical dopant concentration including PSG and BSG while the latter can profile electrically active dopant in silicon. Polished-surface wafers were used for the characterization and three specimens (one with PSG or BSG for D-SIMS, and HF-dipped ones for D-SIMS and for ECV measurements on emitters without the glass layers) were taken from one single wafer for each diffusion condition.

Mono crystalline silicon solar cells were made using these diffusion conditions. The reproducibility of the doping profiles was confirmed by ECV profiling also considering the surface conditions of either polished or textured [12]. Since the wafer material and BSF structure were different between [p-type wafer / phosphor emitter / Al BSF] and [n-type wafer / boron emitter / phosphor BSF], we focused on internal quantum efficiency at shorter wavelength (= blue IQE). We also compared the solar cell performance in which the comparison is not completely fair but practical as the device structure for industrially manufactured product.

Emitter saturation current (J_{0E}) derived from Sinton QSSSPC at high injection levels [13] was also evaluated using a symmetrical sample structure with both sides textured emitter covered with passivation equivalent with the one used for solar cells, which are a PECVD SiN_x film for phosphorus emitters [14] and a stack of chemical oxide / PECVD SiN_x [15,16] for boron emitters.

3. Results and discussion

3.1. Phosphorus doping profiles

Figure 1 shows phosphorus doping profiles of (a) a typical $POCl_3$ process to manufacture industrial solar cells targeting 65 Ω/sq.; and (b) a $POCl_3$ process targeting lighter phosphorus doping by combining oxidation during the drive-in diffusion step with a sheet resistance of 91 Ω/sq. The black curve by D-SIMS indicates phosphorus concentration in the PSG. The red one also by D-SIMS represents the total phosphorus concentration in the actual emitter layer while the blue one by ECV shows the active phosphorus concentration. The profiling depths in emitters were calibrated by measuring the pit depths after each profiling, whose accuracy is within 5%. The PSG thicknesses were calibrated by ellipsometry. The measurements for PSG close to the interface above the emitter were carried out with extra care of slowing down the sputtering to surely stop the digging before reaching the emitter, and the depth step at each profiling point was recalculated considering the decreasing sputtering speed. D-SIMS counted ^{31}P (one and the only stable isotope of phosphorus) ion current comparing with ^{30}Si (a stable isotope representing 3.1% of the Si present) ion with the accuracy within 15%. The concentration in PSG was calculated assuming the PSG is 100% SiO_2 which has Si concentration of 2.20×10^{22} cm^{-3} considering its density is 2.20 g/cm^3. The concentration indicated by ECV is within the accuracy of 10-15%, since it is inversely proportional to the square of the measurement circle area which was calibrated by the pit depth measurement.

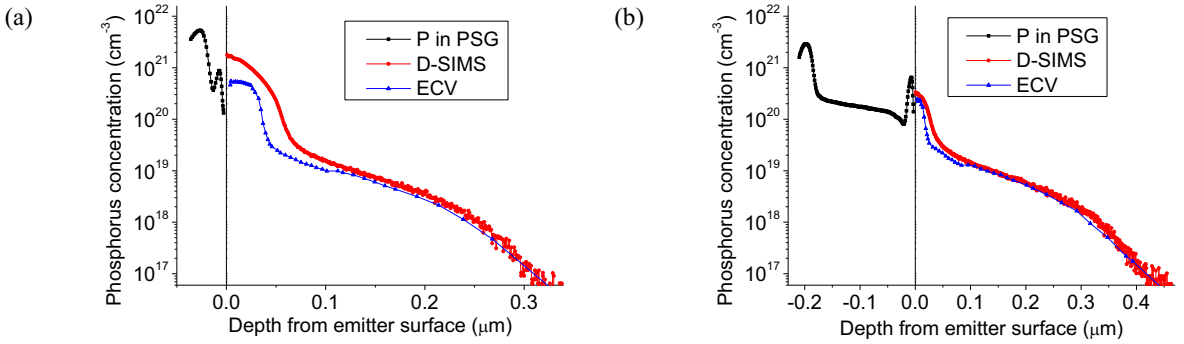

Fig. 1. Phosphorus doping profiles of (a) a typical $POCl_3$ process to manufacture industrial solar cells targeting 65 Ω/sq.; and (b) a $POCl_3$ process targeting lower phosphorus doping by combining oxidation during the drive-in diffusion step with a sheet resistance of 91 Ω/sq.

Two peaks in PSG are observed for each case, near the surface of the PSG and close to the interface above the emitter. Significant concentration difference is demonstrated for each case at the interface. Below the second phosphorus peak in the PSG, the concentration plummets toward the interface down to the level even lower than that of the electrically active concentration measured by ECV. This suggests that phosphorus atoms are strongly segregated towards silicon, which results in a substantial amount of interstitial phosphorus above the solid solubility [6] at thermal equilibrium. The excess phosphorus is represented by the area between the red and the blue curves, which is supposed to be electrically inactive and behave as SRH (Shockley Read Hall) recombination center.

Even below the solid solubility which is $3\text{-}4\times10^{20}$ cm^{-3} [6], the presence of inactive phosphorus is observed both in (a) and in (b) probably due to the thermal inequilibrium of the diffusion / drive-in process. Bentzen *et al.* studied the diffusivity dependence on the concentration [17], which demonstrated the dominance of phosphorus diffusion changes at $1\text{-}2\times10^{19}$ cm^{-3} from interstitial to substitutional toward the diffusion direction. This explains that the D-SIMS and ECV curves are almost identical only below 1×10^{19} cm^{-3}.

3.2. Boron doping profiles

Figure 2 shows boron doping profiles of a BBr_3 tube process targeting 60 Ω/sq. which is similar to that of the n-Pasha solar cells that achieved 20.2% [5] and transferrable to industrial production. Similarly to Fig.1, black, red,

and blue curves indicate that in BSG by D-SIMS, in emitter by D-SIMS and that by ECV, respectively. Since D-SIMS compared ^{11}B (a stable isotope representing 80% of the boron present) with ^{30}Si, the signals were converted into those for all the stable isotopes of boron. The concentration in BSG was calculated in the same way as described above.

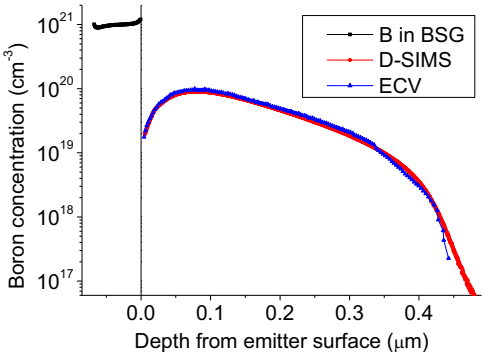

Fig. 2. Boron doping profiles of a BBr_3 tube process targeting 60 Ω/sq., equivalent to that of the n-Pasha solar cells which achieved 20.2% [5] and transferrable to industrial production.

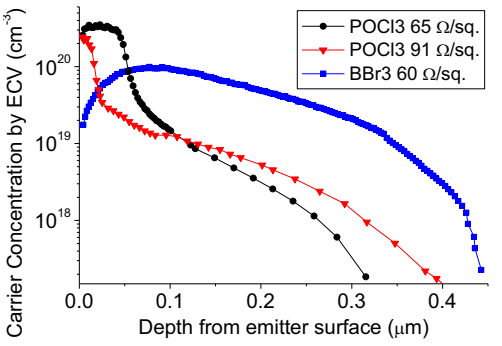

Fig. 3. Re-plotting of the ECV profiles from Fig. 1(a)(b) and Fig. 2 with re-defining the scales.

There is also a significant difference of the boron concentration at the interface between the Si and BSG, but that in the BSG is much higher than in the emitter, so, the opposite that was observed for phosphorus. The boron concentration in BSG looks almost constant and no inactive boron is present in the emitter, demonstrated by the identical curves of D-SIMS and ECV profiles in the emitter. This feature is also enhanced since the process has a short oxidation step during the cooling down from the diffusion temperature to avoid a BRL (boron rich layer) formation in order to remove BSG easily by HF solution [18], therefore the surface concentration is a bit lower though the peak concentration is close to the solid solubility [7]. Segregation of boron atoms towards BSG at the BSG/emitter interface is observed, which seems to cause the absence of electrically inactive boron atoms.

The re-plotted ECV profiles from Fig. 1 (a)(b) and Fig. 2 are shown in Fig. 3 with re-defining the scales.

3.3. Emitter saturation current (J_{0E}) and internal quantum efficiency at shorter wavelength (blue IQE)

The measured emitter saturation currents (J_{0E}) of these emitters were 180 fA/cm², 45 fA/cm², and 97 fA/cm² for the $POCl_3$ 65 Ω/sq., 91 Ω/sq., and BBr_3 60 Ω/sq., respectively. We manufactured solar cells using these emitters with typical industrial processes [5,9,19]. Table 1 shows the average I-V characteristics, although the direct comparison between the $POCl_3$ and the BBr_3 emitters does not give so much scientifically relevant information since the wafer material and the BSF are different. Since the contact optimization of 91 Ω/sq. was not sufficient due to the limited extent of the experiments, the potential efficiency assuming the same FF as the 65 Ω/sq. emitter's is also shown. In order to particularly compare the emitter performance, we focused on the blue IQE spectra which are shown in Fig. 4.

Considering the presence of substantial inactive dopant and much heavier doping near the surface for $POCl_3$ 65 Ω/sq. emitter, it consequently has the largest J_{0E} and the lowest blue IQE. The BBr_3 60 Ω/sq. emitter shows even higher blue IQE than the $POCl_3$ 91 Ω/sq., though both its sheet resistance and J_{0E} are higher. The reason can be because the BBr_3 emitter has lower peak concentration, or no inactive dopant, or better passivation. Though the J_{0E} measurement by QSSPC reflects minority carrier behavior at the open-circuit condition, it may not correctly reflect that for the short-circuit condition in which IQE spectra are measured.

In our analysis on J_{0E} of phosphorus emitters [20], we considered them by separating them in two regions of n^{++} and n^{+} layers, where the former, which is on the surface side, has phosphorus concentration higher than 3×10^{19} cm^{-3} and the latter, which is on the deeper side, has that lower than 3×10^{19} cm^{-3}. Each layer of the n^{++} and n^{+} should have its individual J_{0E}, namely $J_{0E}(n^{++})$ and $J_{0E}(n^{+})$, and J_{0E} of the whole emitter is limited by smaller one of either

$J_{0E}(n^{++})$ and $J_{0E}(n^{+})$ due to the current continuity principle at the series circuit of the n^{++} and n^{+}. It seems the J_{0E} of the $POCl_3$ 91 Ω/sq. emitter at the open circuit condition is determined by $J_{0E}(n^{+})$ because of the lightly doped and relatively deep n^{+} layer resulting in a 10 mV V_{oc} gain from the 65 Ω/sq. emitter. On the other hand, the heavily doped n^{++} layer still causes minority carrier recombination at the short circuit condition, resulting in lower blue IQE.

Table 1. Solar cell performance of mono crystalline Si solar cells using these emitters.

Emitter	J_{sc} (mA/cm^2)	V_{oc} (V)	FF	Eff. (%)	BSF
$POCl_3$ 65 Ω/sq., 180fA/cm^2	36.8	0.626	0.796	18.3	Al paste
$POCl_3$ 91 Ω/sq., 45 fA/cm^2	37.3	0.636	0.770*	18.3 (18.9**)	Al paste
BBr_3 60 Ω/sq., 97 fA/cm^2	39.2	0.652	0.783	20.0	$POCl_3$

* Contact optimization was not sufficient due to the limited extent of the experiments

** Potential efficiency assuming the same FF can be realized as the 65 Ω/sq. emitter's.

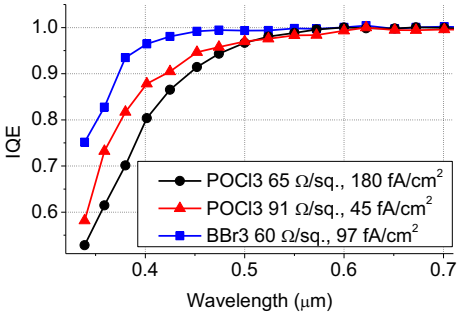

Fig. 4. IQE spectra at shorter wavelength

In the same analysis [20], we also pointed out the necessity of heavily doped surface for phosphorus emitters because the width of the depletion layer induced on the n^{++}-emitter surface by the high Schottky barrier of silver should be as thin as possible to increase the number of electrons which tunnel through the depletion layer to the Ag metal contact. On the other hand, aluminum in Ag/Al paste used for the boron emitter contact [5,19] can be assumed to form an Al:Si eutectic which is expected to help extraction of holes at p^{+}-Si surface towards the metal contact. This is very likely to be the reason why the boron emitter has sufficiently low contact resistance without such a heavily doped surface as the phosphorus emitter must have. The absence of heavy doping above 1×10^{20} cm^{-3} could work positively for the higher blue IQE of the BBr_3 emitter.

The effect of the lowest J_{0E} of $POCl_3$ 91 Ω/sq. is reflected as a V_{oc} gain of 10 mV from 65 Ω/sq. one. It suggests that decreasing J_{0E} of the BBr_3 emitter will still improve the V_{oc}.

4. Conclusions

A boron emitter that is transferrable to mass production and achieved 20.2% [5] (20.0% as the average) was compared to two phosphorus emitters of industrial standard whose efficiency is 18.3% and of reduced phosphorus concentration whose potential efficiency is 18.9%, on the viewpoints of the doping profiles, J_{0E}, and blue IQE. We focused on the interface between the dopant source (BSG or PSG) and the emitter, and presumed that the difference of the segregating direction of the dopant causes the presence or the absence of the inactive dopant. We found inactive phosphorus is still present even down to 1×10^{19} cm^{-3} also for lightly doped diffusion while no inactive boron is detected. The boron emitter showed the largest blue IQE which suggests minority carrier recombination in the short circuit condition is the lowest. On the other hand, the 10 mV V_{oc} gain of the phosphorus emitters by

decreasing J_{0E} from 180 to 45 fA/cm^2 implied the possibility of V_{oc} improvement for the boron emitter by reducing J_{0E} which is 97 fA/cm^2 at present.

Acknowledgements

The authors are grateful to Dr. Peter Breimer and Dr. Jurgen van Berkum at Philips Innovation Services for the careful D-SIMS measurements and the useful discussion on the calibration.

References

[1] Schmidt J, Aberle AG, Hezel R, Investigation of carrier lifetime instabilities in Cz-grown silicon, Proc 26th IEEE Photovolaic Specialist Conference: Anaheim: California: USA; 1997. p.13-8.
[2] MacDonald D, Geerligs LJ, Recombination activity of interstitial iron and other transition metal point defects in p- and n-type crystalline silicon, Appl Phys Lett 2004;85:4061-3.
[3] Smith DD, Cousins PJ, Masad A, Westerberg S, Defensor M, Ilaw R, Dennis T, Daquin R, Bergstrom N, Leygo A, Zhu X, Meyers B, Bourne B, Shields M, Rose D, SunPower's Maxeon Gen III solar cell: High efficiency and energy yield, Proc 39th IEEE Photovolaic Specialist Conference: Tampa: Florida: USA; 2013. p.908-13.
[4] Taguchi M, Yano A, Tohoda S, Matsuyama K, Nakamura Y, Nishiwaki T, Fujita K, Maruyama E, 24.7% record efficiency HIT solar cell on thin silicon wafer, IEEE Journal of Photovoltaics 2014;4:96-9.
[5] Romijn IG, Van Aken BB, Anker J, Barton PC, Gutjahr A, Komatsu Y, Koppes M, Kossen EJ, Lamers MWPE, Saynova DS, Tool CJJ, Zhang Y, Industrial cost effective n-Pasha solar cells with >20% efficiency, Proc 28th European Photovoltaic Solar Energy Conference and Exhibition: Paris: France: 2013. p. 736-40.
[6] Kooi E, Formation and composition of surface layers and solubility limits of phosphorus during diffusion in silicon, J Electrochemical Society 1964;111:1383-7.
[7] Vick GL, Whittle KM, Solid solubility and diffusion coefficients of boron in silicon, J Electrochemical Society 1969;116:1142-4.
[8] Komatsu Y, Mihailetchi VD, Geerligs JL, Van Dijk B, Rem JB, Harris M, Homogeneous p^+ emitter diffused using boron tribromide for record 16.4% screen-printed large area n-type mc-Si solar cell, Solar Energy Materials and Solar Cells 2009;93:750-2.
[9] Komatsu Y, Galbiati G, Lamers MWPE, Venema PR, Harris M, Stassen AF, Meyer C, Van den Donker MN, Weeber AW, Innovative diffusion processes for improved efficiency on industrial solar cells approached by doping profile manipulation, Proc 24th European Photovoltaic Solar Energy Conference and Exhibition: Hamburg: Germany: 2009. p. 1063-7.
[10] http://www.innovationservices.philips.com/
[11] http://www.wepcontrol.com/cv-profiler/
[12] Komatsu Y, Harata D, Schuring EW, Vlooswijk AHG, Katori S, Fujita S, Venema PR, Cesar I, Calibration of electrochemical capacitance-voltage method on pyramid texture surface using scanning electron microscopy, Energy Procedia 2013;38:94-100.
[13] Kane DE, Swanson RM, Measurement of the emitter saturation current by a contactless photoconductivity decay method, Proc 18th IEEE Photovolaic Specialist Conference: Las Vegas: Nevada: USA: 1985. p. 578-83.
[14] Romijn IG, Soppe WJ, Rieffe HC, Sinke WC, Weeber AW, Passivating multi crystalline Si solar cells using SiNx:H, Proc 15th Workshop on Crystalline Silicon Solar Cells & Modules: Materials and Processes: Vail: Colorado: USA: 2005. p.80-7.
[15] Komatsu Y, Geerligs LJ, Mihailetchi VD, Method of manufacturing crystalline silicon solar cells with improved surface passivation, International patent application WO2008/039067.
[16] Mihailetchi VD, Komatsu Y, Geerligs LJ, Nitric acid pretreatment for the passivation of boron emitters for n-type base silicon solar cells, Appl Phys Lett 2008;92:063510.
[17] Bentzen A, Holt A, Christensen JS, Svensson BG, High concentration in-diffusion of phosphorus in Si from a spray-on source, J Appl Phys 2006:99:064502.
[18] Vlooswijk AHG, Venema PR, Komatsu Y, Boron compounds, production and application: Nova Science Publishers; 2010. chapter 16.
[19] Romijn IG, Gutjahr A, Saynova - Oosterling DS, Anker J, Kossen EJ, Tool CJJ, Cost effective n-Pasha solar cells with efficiency above 20%, Photovoltaics International 2013;20:33-40.
[20] Komatsu Y, Koorn M, Vlooswijk AHG, Venema PR, Stassen AF, Efficiency improvement by deeper emitter with lower sheet resistance for uniform emitters, Energy Procedia 2011;8:515-20.